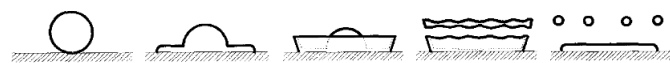


Tropfendynamik in Wandnähe – Möglichkeiten und Limitierungen von grenzflächenauflösenden Simulationen

Drop dynamics near walls – achievements and limitations of interface-resolving simulations

Jahrestreffen der ProcessNet-Fachgruppen Computational Fluid Dynamics und Gasreinigung, Bamberg, 10. – 11. März 2020

C. Mundo, M. Sommerfeld, C. Tropea, *Int. J. Multiph. Flow* 21 (1995) 151-173



Schematic view of the splashing process.

Dr.-Ing. Martin Wörner

Karlsruher Institut für Technologie (KIT)

Institut für Katalysatorforschung und -technologie (IKFT)



Schematic view of the deposition process.

Motivation

- Technical applications where droplet-wall interactions are important
 - spray cooling of hot surfaces or in nuclear reactors
 - spray painting and spray coating (e.g., tablets in pharmaceutical industry)
 - spray based cleaning methods for semiconductor manufacturing
 - fire suppression (sprinkler)
 - agriculture (irrigation, crop dusting)
 - droplet-impact erosion on turbine blades
 - inkjet printing
 - aircraft-related applications
 - internal combustion engines
- } *droplet impact speeds up to 50 m/s*
- In some applications spreading is desirable (coating, inkjet-printing, ...) while in other splashing is desirable to improve the efficiency of evaporation and mixing
 - *The most fundamental process which needs to be understood is the interaction of a single droplet with a dry or wetted solid wall*

Outline

- Introduction
- Droplet impact on a dry surface
 - Smooth surface
 - Structured surfaces
- Droplet impact on film of the same liquid
- Droplet impact on film of a different liquid
 - Immiscible liquids
 - Miscible liquids



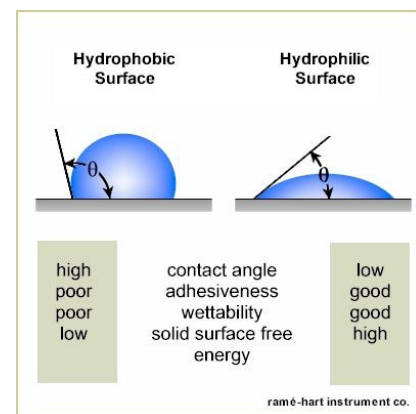
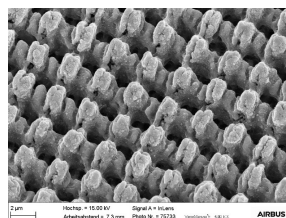
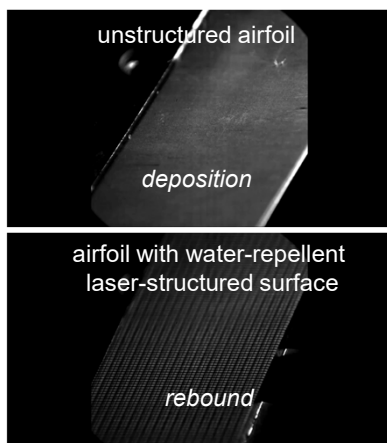
- Conclusions

For each case the relevant physical phenomena are discussed and an illustrative computational example from literature or own work is given.

The presentation is limited to hydrodynamics without heat transfer.

Dry surface – deposition and rebound

- Fraunhofer Research News 3–2020: A fast, ecofriendly way of de-icing aircrafts

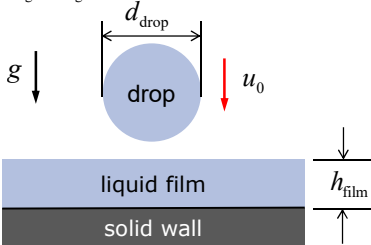


<https://www.fraunhofer.de/en/press/research-news/2020/march/a-fast-ecofriendly-way-of-de-icing-aircrafts.html>

Definitions and classification

$\rho_{\text{drop}}, \mu_{\text{drop}}, \sigma$

$\rho_{\text{gas}}, \mu_{\text{gas}}$

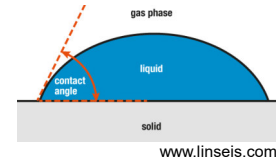


$$We = \frac{\rho_{\text{drop}} d_{\text{drop}} u_0^2}{\sigma}, Oh = \frac{\mu_{\text{drop}}}{\sqrt{\rho_{\text{drop}} \sigma d_{\text{drop}}}} = \frac{\sqrt{We}}{Re}, Fr = \frac{u_0^2}{gd_{\text{drop}}} = \frac{We}{Bo}$$

$$\hat{h} = \frac{h_{\text{film}}}{d_{\text{drop}}}, \hat{R}_a = \frac{R_a}{d_{\text{drop}}}, \hat{L}_a = \frac{L_a}{d_{\text{drop}}}, \hat{\rho}_{\text{gas}} = \frac{\rho_{\text{gas}}}{\rho_{\text{drop}}} \ll 1, \hat{\mu}_{\text{gas}} = \frac{\mu_{\text{gas}}}{\mu_{\text{drop}}} \ll 1$$

Characteristics of the solid wall

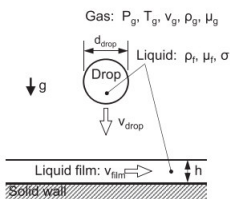
- R_a = mean value of wall roughness
- L_a = length scale of wall roughness
- Wettability (static contact angle θ_{stat})



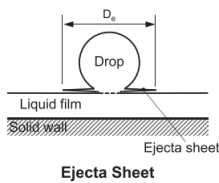
	dry wall	thin film	liquid film	shallow pool	deep pool
Impact depends on	$\hat{h} = 0$	$\hat{L}_a < \hat{h} < 3\hat{R}_a^{0.16}$	$3\hat{R}_a^{0.16} < \hat{h} < 1.5$	$1.5 < \hat{h} < 4$	$\hat{h} \gg 4$
Wall features	++	++	+	-	-
Film thickness	-	+	+	+	-

C. Tropea, M. Marengo, The impact of drops on walls and films, *Multiphase Science and Technology* 11 (1999) 19-36

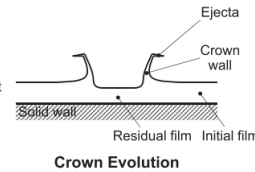
Phenomena for drop impact on liquid film



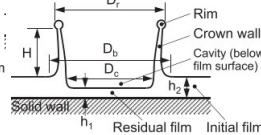
Drop Approaching Film



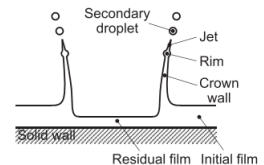
Ejecta Sheet



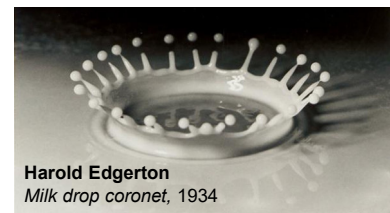
Crown Evolution



Crown Formation without Splashing



Crown Splashing



Harold Edgerton
Milk drop coronet, 1934

$$\hat{\rho}_f = \frac{\rho_{\text{film}}}{\rho_{\text{drop}}}, \hat{\mu}_f = \frac{\mu_{\text{film}}}{\mu_{\text{drop}}}, \hat{\sigma}_f = \frac{\sigma_{\text{film}}}{\sigma_{\text{drop}}}$$

G. Liang, I. Mudawar, Review of mass and momentum interactions during drop impact on a liquid film, *Int. J. Heat Mass Transf.* 101 (2016) 577-599

Governing equations

- One-field Navier-Stokes equations for two incompressible, immiscible Newtonian fluids

$$\rho \partial_t \mathbf{u} + \rho \nabla \cdot (\mathbf{u} \otimes \mathbf{u}) = -\nabla p + \nabla \cdot [\mu (\nabla \mathbf{u} + (\nabla \mathbf{u})^T)] + \rho \mathbf{g} + \mathbf{f}_\sigma, \quad \nabla \cdot \mathbf{u} = 0$$

- Numerical methods for interface evolution to determine $\rho = \rho(\mathbf{x}, t)$, $\mu = \mu(\mathbf{x}, t)$, $\mathbf{f}_\sigma = \mathbf{f}_\sigma(\mathbf{x}, t)$

- Geometric volume-of-fluid method (sharp interface)

- Discontinuous phase indicator (liquid volume fraction f)

$$\partial_t f + \nabla \cdot (f \mathbf{u}) = 0$$

- Excellent volume conservation, high accuracy only for Cartesian grids

- Level-set method (sharp interface)

- Smooth phase indicator (signed distance from interface ϕ)

$$\partial_t \phi + \mathbf{u} \cdot \nabla \phi = 0$$

- Problems with mass conservation \rightarrow re-initialization

$$\mathbf{f}_\sigma = \sigma \kappa \delta_{if} \mathbf{n}_{if}$$

- Phase field method (diffuse interface)

- Interface thickness ε is input parameter formally decoupled from grid resolution

- Diffusive mechanism for motion of the contact line at a no-slip wall

$$\partial_t C + \nabla \cdot (C \mathbf{u}) = M \nabla^2 \phi$$

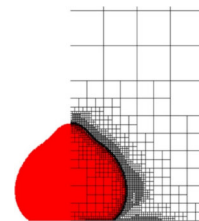
- Surface tension is modelled as energy not as force

- Problems with boundedness and volume conservation

$$\mathbf{f}_\sigma = -C \nabla \phi_m$$

Gerris Flow Solver

- Open-source code develop by S. Popinet and coworkers (<http://gfs.sf.net>)
- Geometric volume-of-fluid (VOF) method (PLIC = Piecewise Linear Interface Calculation)
- Finite volume method with dynamic adaptive (octree) mesh refinement (AMR) on Cartesian grids
- Balanced discretization of surface tension and pressure forces in combination with accurate height-function based curvature computation \rightarrow very low spurious currents
- Domain decomposition based parallelism with dynamic load balancing
- Schemes are second order accurate in both space and time
- Cut-cell method for complex solid boundaries
- Mesh-dependent static contact angle model by default
- Team now focuses on development of *Basilisk* code (<http://basilisk.fr/>)
 - Both codes are compared for drop impact on a liquid film by Wu et al. (2020)
 - Similar results but Basilisk shows much higher computational efficiency due its superior parallelization



- S. Popinet, Gerris: a tree-based adaptive solver for the incompressible Euler equations in complex geometries, *J. Comput. Phys.* **190** (2003) 572-600
- S. Popinet, An accurate adaptive solver for surface-tension-driven interfacial flows, *J. Comput. Phys.* **228** (2009) 5838-5866
- S. Wu, J. Zhang, Q. Xiao, M.-J. Ni, Comparison of two interfacial flow solvers: Specific case of a single droplet impacting onto a deep pool, *Comput. Math. Appl.*, in press

Computer code *phaseFieldFoam*



- Code development
 - Dr. Xuan Cai (KIT, now at Bosch), Dr. Holger Marschall (TU Darmstadt)
 - Dr. Nima Samkhaniani (KIT), Milad Bagheri (TU Darmstadt), ...
- Implementation in OpenFOAM
 - foam-extend-4.0
 - Finite volume method on general grids
 - Cahn-Hilliard or Allen-Cahn approach
 - Dynamic adaptive mesh refinement
 - Code shall be released to the public in the medium term
- Validation and application for various test cases
 - Typical mesh resolution $\Delta x = \varepsilon / 2 \rightarrow 8$ cells in diffuse interface

📄 X. Cai, H. Marschall, M. Wörner, O. Deutschmann, *Chem. Eng. Technol.* **38** (2015) 1985-1992
📄 X. Cai, M. Wörner, H. Marschall, O. Deutschmann, *Emission Control Science and Technology* **3** (2017) 289-301
📄 M. Börnhorst, X. Cai, M. Wörner, O. Deutschmann, Maximum spreading of urea water solution during drop impingement, *Chem. Eng. Technol.* **42** (2019) 2419-2427
📄 V. Fink, X. Cai, A. Stroh, R. Bernard, J. Kriegseis, B. Frohnäpfel, H. Marschall, M. Wörner, Drop bouncing by micro-grooves, *Int. J. Heat Fluid Flow* **70** (2018) 271-278



Drop impact on dry surface

Challenge – Modeling of contact line motion

- For a moving contact line, the apparent contact angle may differ from the static contact angle $\theta_{\text{stat}} \rightarrow$ *dynamic* contact angle θ_{dyn}
- Hydrodynamic model (Voinov 1976, Cox 1986)
 - Slip length L_{slip} needs to be specified

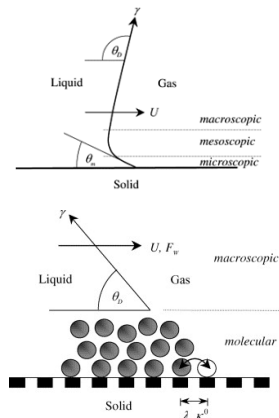
$$\theta_{\text{dyn}} = (\theta_{\text{stat}}^3 + 9C \cdot Ca_{\text{cl}})^{1/3}, \quad C = \ln(L_{\text{macro}} / L_{\text{slip}}), \quad Ca_{\text{cl}} = \frac{\mu_{\text{drop}} U_{\text{cl}}}{\sigma}$$

- Molecular dynamic model (Blake 2006)
 - Molecule jump frequency (κ) and jump length (λ) need to be specified

$$\cos \theta_{\text{dyn}} = \cos \theta_{\text{stat}} - \frac{k_B T}{\mu \kappa \lambda} Ca_{\text{cl}}$$

- Inertia dominated flow stages are largely unaffected by changes in c. a.
- Contact line pins at topological or chemical heterogeneities on the wall giving rise to *contact angle hysteresis*

O.V. Voinov, Hydrodynamics of wetting, *Fluid Dynamics* **11** (1976) 714-721
 R.G. Cox, The Dynamics of the Spreading of Liquids on a Solid-Surface. Part 1. Viscous-Flow, *J. Fluid Mech.* **168** (1986) 169-194
 T.D. Blake, The physics of moving wetting lines, *J. Colloid Interf. Sci.* **299** (2006) 1-13
 Y. Sui, H. Ding, P.D.M. Spelt, Numerical simulations of flows with moving contact lines, *Annu. Rev. Fluid Mech.* **46** (2014) 97-119



Impact on smooth dry surface

- 3D level-set simulations
- $d_{\text{drop}} = 1.86 \text{ mm}$, $u_0 = 2.98 \text{ m/s}$
- Equilibrium contact angle $\theta_{\text{stat}} = 163^\circ$ yields splashing in agreement with exp.
- A value $\theta_{\text{stat}} = 40^\circ$ in combination with a dynamic c. a. model can induce splash.

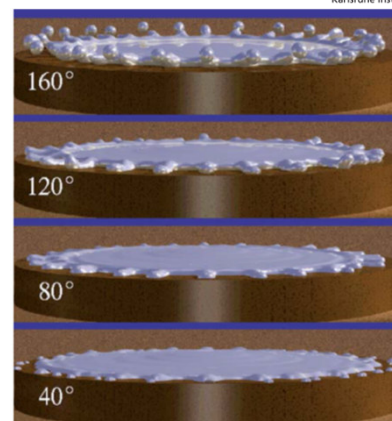
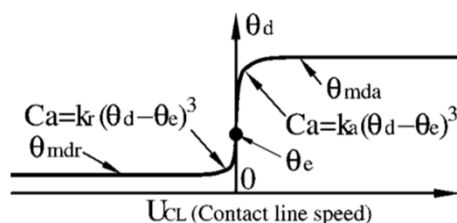
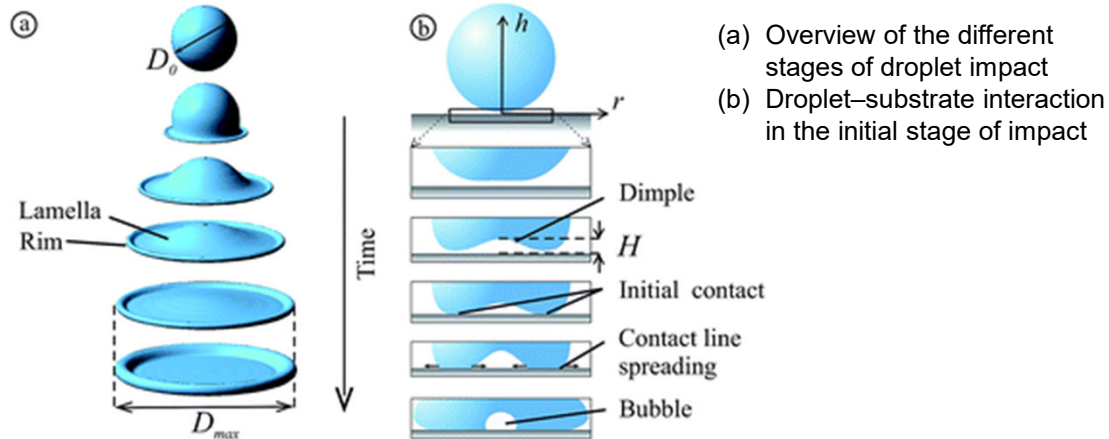


Fig. 4 Numerical results when the maximum dynamic advancing angle θ_{mda} is varied from 160° to 40° . The spreading speeds are different depending on θ_{mda} . Therefore the time of each snapshot is different (160° : 1.6 ms, 120° : 1.36 ms, 80° : 1.2 ms, 40° : 1.2 ms).

K. Yokoi, Numerical studies of droplet splashing on a dry surface: triggering a splash with the dynamic contact angle, *Soft Matter* **7** (2011) 5120-5123

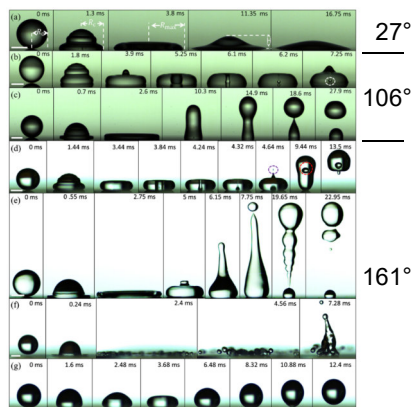
Bubble entrapment



C.W. Visser, P.E. Frommhold, S. Wildeman, R. Mettin, D. Lohse, C. Sun, Dynamics of high-speed micro-drop impact: numerical simulations and experiments at frame-to-frame times below 100 ns, *Soft Matter* **11** (2015) 1708-1722

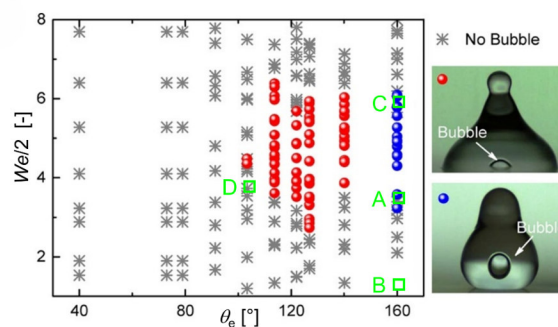
Drop impact on dry (hydrophobic) surfaces

Experiments Lin et al. (2018)



Regime map on bubble entrapment behavior

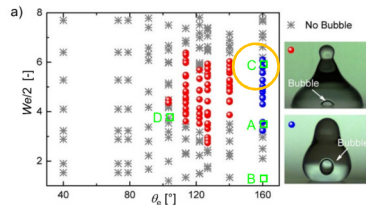
Chen et al. (2017)



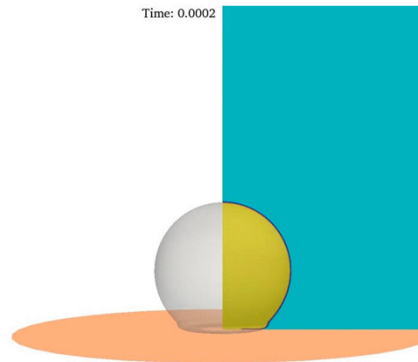
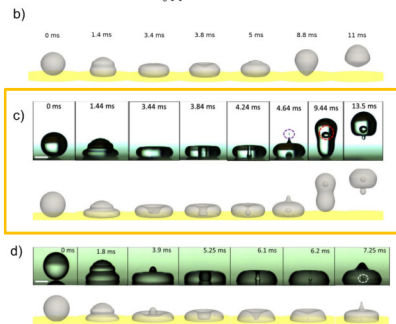
S.J. Lin, B.Y. Zhao, S. Zou, J.W. Guo, Z. Wei, L. Chen, Impact of viscous droplets on different wettable surfaces: Impact phenomena, the maximum spreading factor, spreading time and post-impact oscillation, *J. Colloid Interf. Sci.* **516** (2018) 86-97

L. Chen, L. Li, Z.-D. Li, K. Zhang, Submillimeter-sized bubble entrapment and a high-Speed jet emission during droplet impact on solid surfaces, *Langmuir* **33** (2017) 7225-7230

Numerical results by *phaseFieldFoam* for case C

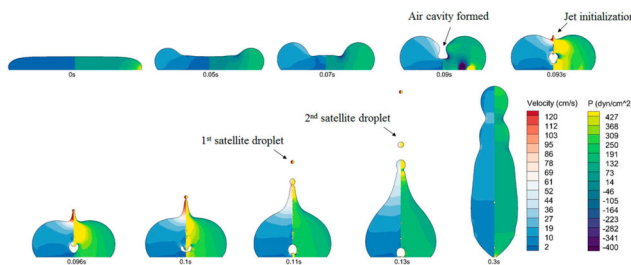


- Water drop impact on superhydrophobic surface ($\theta_{stat} = 161^\circ$)
 - $d_{drop} = 2 \text{ mm}$, $u_0 = 0.65 \text{ m/s}$, $We = 11.7$, $Re = 1440$
 - bubble encapsulation in impact center \rightarrow floating bubble
 - see presentation of Nima Samkhaniani this afternoon 14:10

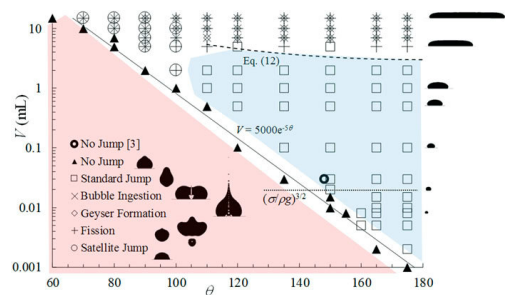


Jumping of an initially flat liquid puddle

- A puddle can spontaneously jump from a nonwetting surface when gravity is nullified (drop tower)
- Extensive validated axisymmetric numerical simulations using modified version of *Gerris* code
 - Mesh refinement level 11 = 247 h vs 7 h for level 9 (2.0 GHz processor with 16 GB RAM)



Velocity (left) and pressure (right) contours of the puddle jump process for $V_{drop} = 10 \text{ ml}$ and $\theta_{stat} = 135^\circ$

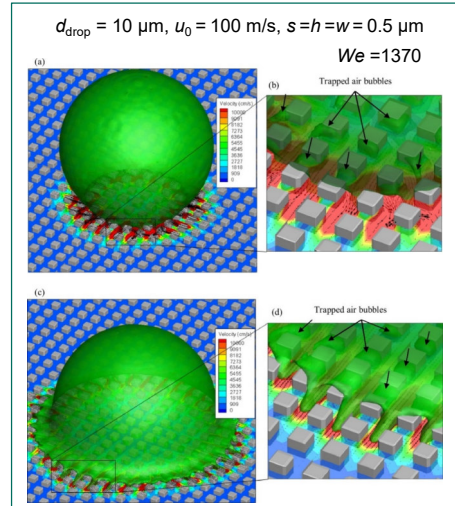
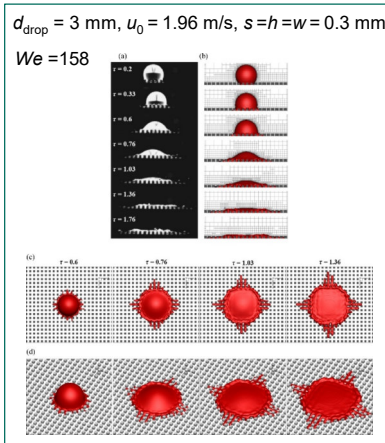
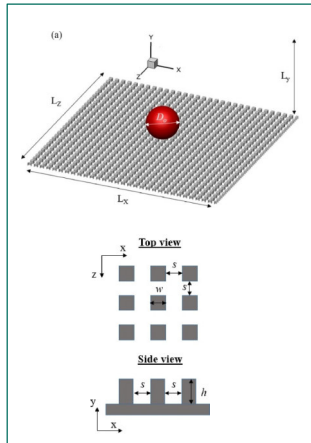


Numerical puddle jump regime map

A. Avhad, H. Tan, T. Al-Jubaree, L. Torres, M. Weislogel, A numerical investigation of puddle jumping, *Phys. Fluids* **32** (2020) 012109

Impact on structured dry surface – splashing

- Gerris modified for contact angle treatment
- Drop impact on dry microstructured surface, $\theta_{stat} = 90^\circ$



H. Tan, Numerical study on splashing of high-speed microdroplet impact on dry microstructured surfaces, *Comput. Fluids* **154** (2017) 142-166

Impact on structured dry surface – bouncing

- Drop impact experiments on hydrophobic PDMS substrate
 - Flat surface: $\theta = 100.3^\circ$, mean roughness depth $R_a = 0.56 \text{ }\mu\text{m}$
- Water drop with diameter $d_{drop} = 2.1 \text{ mm}$
- Drop impact velocity $u_0 = 0.62 \text{ m/s}$ ($We = 11$, $Re = 1300$)

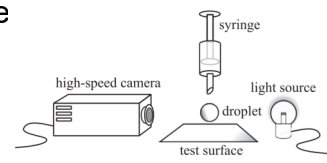
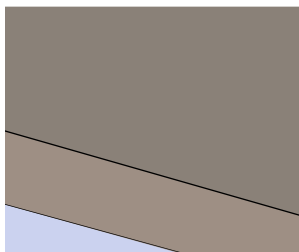
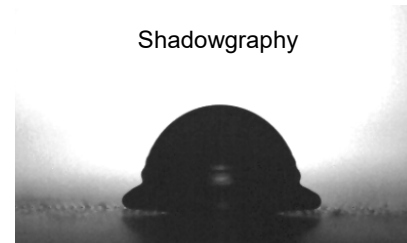
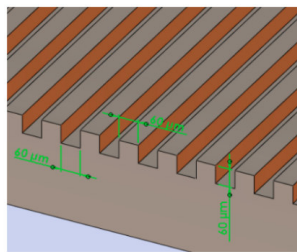


Fig. 1. Schematic of the shadowgraphy set-up.

Flat Surface
 Deposition

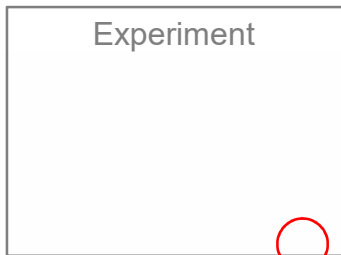
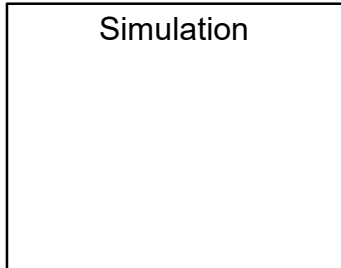


Surface with micro-grooves (60 μm)
 Rebound

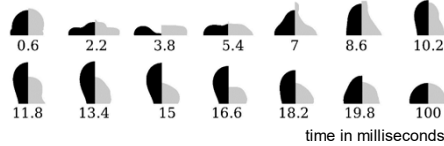


V. Fink, X. Cai, A. Stroh, R. Bernard, J. Kriegseis, B. Frohnappfel, H. Marschall, M. Wörner, Drop bouncing by micro-grooves, *Int. J. Heat Fluid Flow* **70** (2018) 271-278

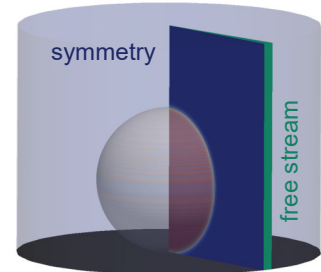
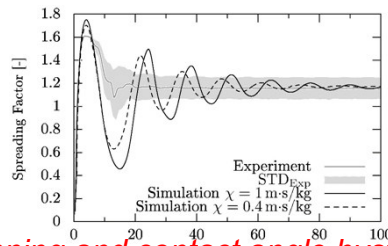
Flat surface – comparison *phaseFieldFoam*



Instantaneous drop shape



Spreading factor



no-slip wall, $\theta_{stat} = 100.3^\circ$

$$\Delta x = 10 \mu\text{m}$$

$$\varepsilon = 22 \mu\text{m}$$

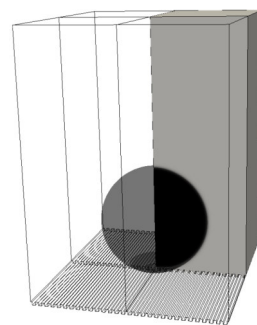
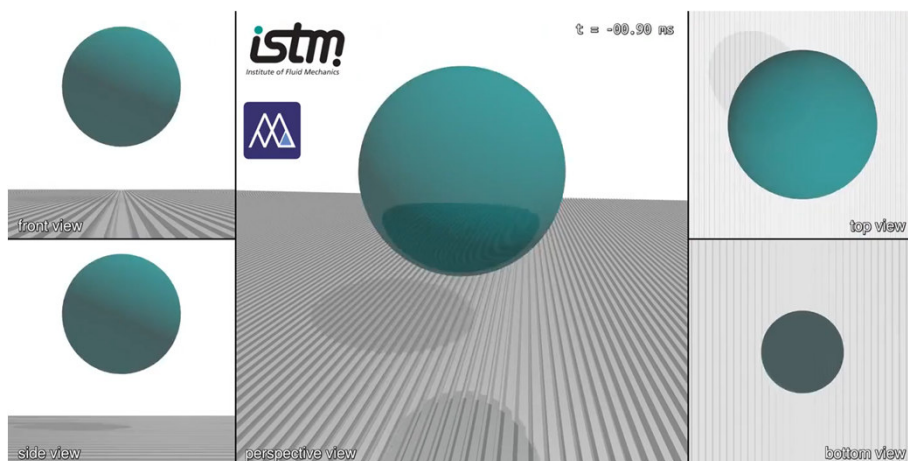
$$4\varepsilon / \Delta x = 8.8$$

$$d_{drop} / \Delta x = 210$$

$$Cn = \varepsilon / d_{drop} = 0.0105$$

Pinning and contact angle hysteresis

Impact on structured surface (simulation)

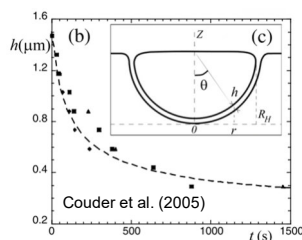


- 18 million mesh cells (no AMR at that time)
- 800,000 CPUh (500 CPU cores)

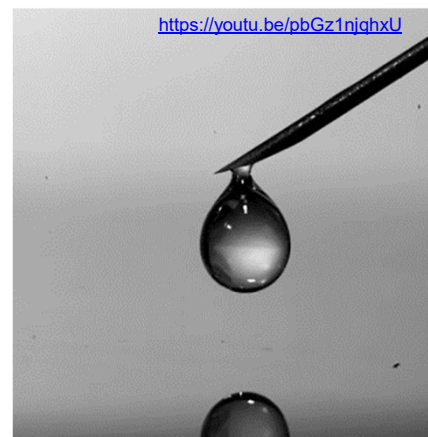
Drop impact on film of identical liquid

Drop bouncing on liquid film or pool

- Droplet bouncing on liquid surfaces frequently occurs for low Weber number impacts
- Bouncing results from the formation of a layer of gas trapped between the droplet and the liquid surface
- The van der Waals forces rupture this layer when the thickness is reduced to ~ 100 nm



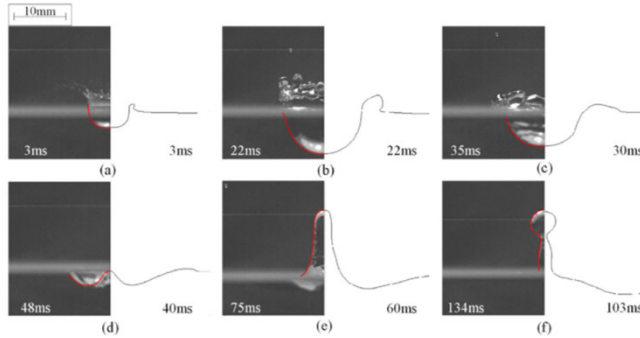
Drop bouncing from a liquid surface has not been reproduced by DNS so far to my knowledge



- Y. Couder, E. Fort, C.H. Gautier, A. Boudaoud, From bouncing to floating: Noncoalescence of drops on a fluid bath, *Phys. Rev. Lett.* **94** (2005) 177801
- I.S. Klyuzhin, F. Ienna, B. Roeder, A. Wexler, G.H. Pollack, Persisting Water Droplets on Water Surfaces, *J. Phys. Chem. B* **114** (2010) 14020-14027
- X. Tang, A. Saha, C.K. Law, C. Sun, Bouncing drop on liquid film: Dynamics of interfacial gas layer, *Phys. Fluids* **31** (2019)

Shallow/deep pool: crater formation and central splash

- Drop impact creates a crater, which expands and then retracts due to capillary forces and gravity
 - For relatively low We , the impact generates a set of circular waves expanding on the film
 - At high Weber numbers, retraction of the crater can lead to generation of central jet which may break



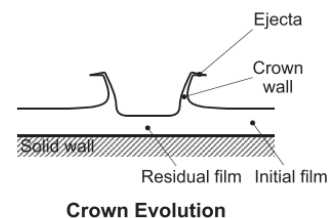
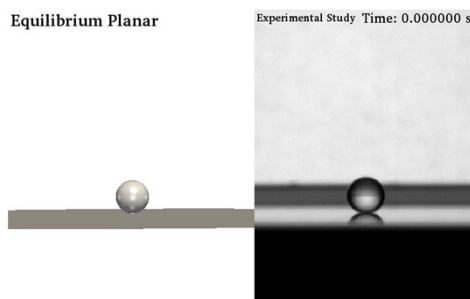
Qualitative comparison between experimental (left) and numerical (right) results for $We = 485$. Numerical simulations performed with VOF method of Fluent.

N.P. van Hinsberg, M. Budakli, S. Gohler, E. Berberovic, I.V. Roisman, T. Gambaryan-Roisman, C. Tropea, P. Stephan, Dynamics of the cavity and the surface film for impingements of single drops on liquid films of various thicknesses, *J. Colloid Interf. Sci.* **350** (2010) 336-343
 H. Ma, C. Liu, X. Li, H. Huang, J. Dong, Deformation characteristics and energy conversion during droplet impact on a water surface, *Phys. Fluids* **31** (2019) 062108

Axisymmetric crown formation without splash

- Experiments by B. Stumpf (TU Darmstadt)
 - Silicon oil (5 cSt), $d_{\text{drop}} = 1.5 \text{ mm}$, $u_0 = 3 \text{ m/s}$, $h_{\text{film}} = 0.5 \text{ mm}$, $We = 701$, $Oh = 0.029$, $Re = 900$
- Simulations with *phaseFieldFoam* by M. Bagheri (TU Darmstadt)
 - Relaxation model for mixing energy parameter for dynamic interface generation

SFB/Transregio 150
 Turbulente, chemisch reagierende
 Mehrphasenströmungen in Wandnähe

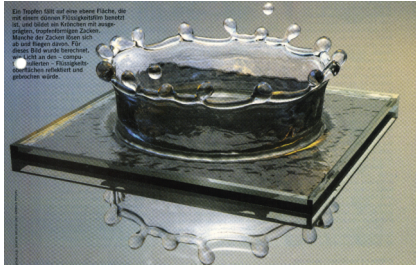


- Goal:** benchmark for time evolution of characteristic dimensions in axisymmetric crown formation

Crown formation with splashing

Rieber & Frohn (1999)

- Geometric PLIC-VOF method
 - FS3D code, now further developed by groups of D. Bothe and B. Weigand
- 320³ cells (2 symmetry planes)
- $We = 250$, $Oh = 0.0014$, $h_{film}/d_{drop} = 0.116$



M. Rieber, A. Frohn, *Int. J. Heat Fluid Flow* **20** (1999) 455-461
 J.O. McCaslin, O. Desjardins, *J. Comput. Phys.* **262** (2014) 408-426

McCaslin & Desjardin (2014)

- Conservative level-set method
- Local re-initialization of level-set function for improvement of volume-conservation
- $We = 598$, $512 \times 1024 \times 1024$ cells

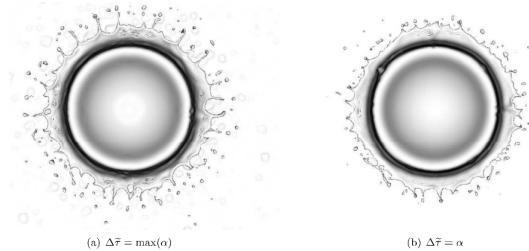


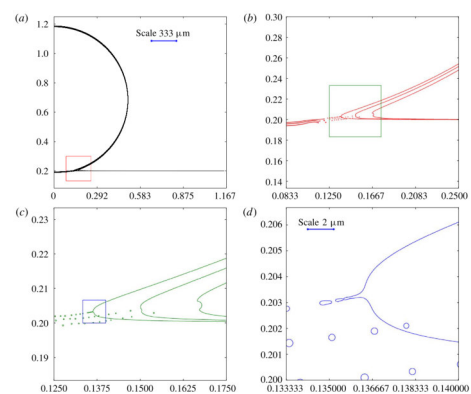
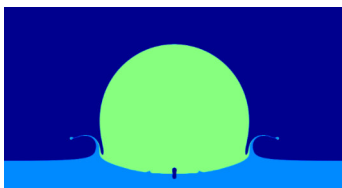
Fig. 21. Effect of local re-initialization on the formation of the liquid sheet at $T = 0.7$.

Studies showing grid depend. of crown splash

K. Yokoi, *J. Sci. Comput.* **35** (2008) 372-396.
 S. Shin, J. Chergui, D. Juric, *J. Mech. Sci. Techn.* **31** (2017) 1739-1751

Ejecta sheet and prompt splash at large We

- Jetting in neck region where the drop meets the film
- The "ejecta sheet" originates from liquid film and its initial speed can be more than $10u_0$
- Instability of ejecta sheet results in prompt ($t \ll d_{drop}/u_0$) generation of secondary droplets
- Numerical simulations by Josserand et al. (2016)
 - Gerris, axisymmetric, bubble entrapment, $d = 2$ mm
 - "Realistic 3D simulations of drop impact at short times are as yet hard to obtain"

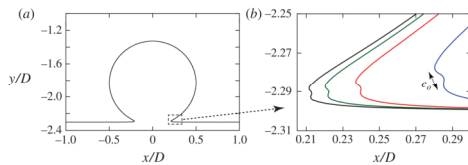


Successive zooms of the interface around the time of jet formation for $We = 500$. Scale $2 \mu m = 20 \Delta x$.



S.T. Thoroddsen, *J. Fluid Mech.* **451** (2002) 373-381
 L.V. Zhang, J. Toole, K. Fezzaa, R.D. Deegan, *J. Fluid Mech.* **690** (2012) 5-15
 C. Josserand, P. Ray, S. Zaleski, *J. Fluid Mech.* **802** (2016) 775-805

Growth of liquid rim at higher We

- Simulations by Agbaglah & Deegan (2014)
 - Gerris code, axisymmetric, $h_{\text{film}}/d_{\text{drop}} = 0.2$
 - Mesh $2^{13} \times 2^{13}$ (8192×8192), $\Delta x = d_{\text{drop}}/1638$
 - Simulations for 30 different combinations of We (200–1000) and Re (500–4000)



- Comparison with experiments by Zhang (2012)
 - Right: We = 324, Re = 2191, $t = 335 \mu\text{s}$
 - Edge of crown becomes unstable and breaks into small droplets (not covered by simulation)

 L.V. Zhang, J. Toole, K. Fezzaa, R.D. Deegan, *J. Fluid Mech.* **690** (2012) 5-15
 G. Agbaglah, R.D. Deegan, *J. Fluid Mech.* **752** (2014) 485-496

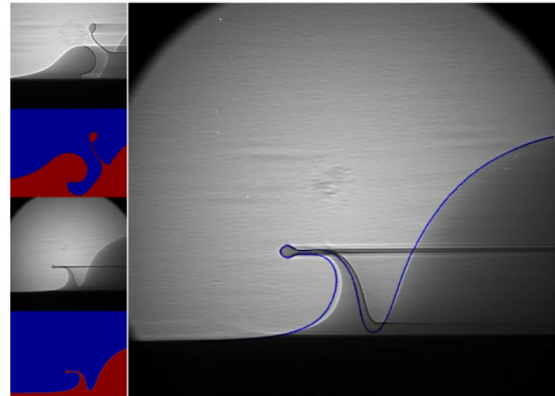
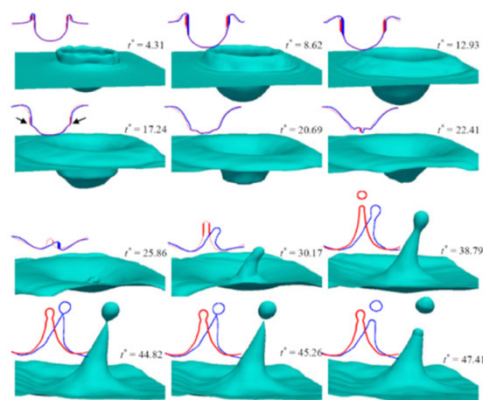






FIGURE 2. (Colour online) Validation. Left: Comparison of experimental profiles obtained using high-speed X-ray imaging and numerical simulations for $h = 5$, $We = 451$ and $Re = 710$ (top) and $h = 0.2$, $We = 324$ and $Re = 2191$ (bottom). Right: Superimposed simulation (line, shown in blue online) and experimental profiles at $t = 335 \mu\text{s}$ ($tU/D = 0.468$) for $h = 0.2$, $We = 324$, $Re = 2191$.

Oblique impact and impact on moving liquid film

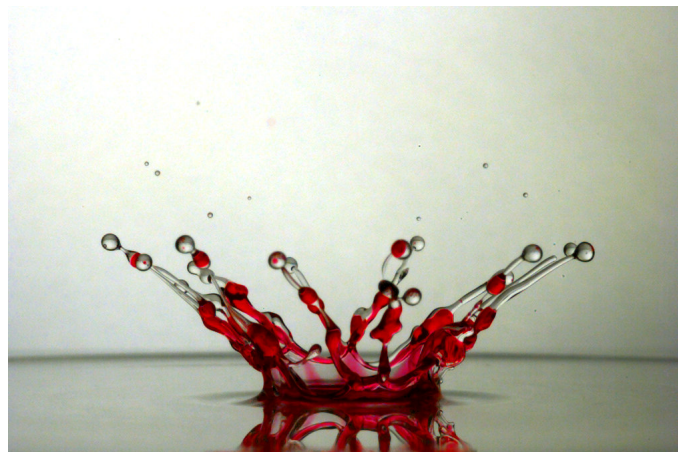
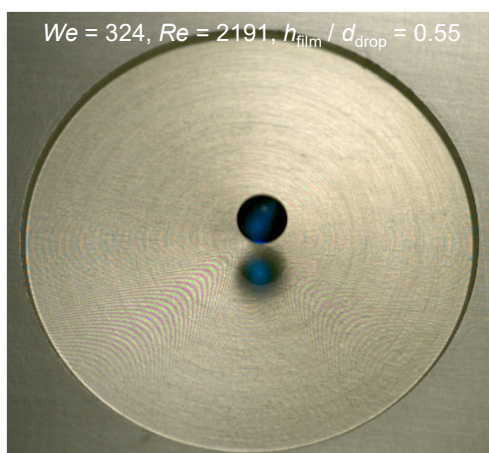
- Oblique impact on static liquid film
 - Chai et al. (2017), level-set method, 2D planar simulations
- Impact on moving liquid film
 - Liu et al. (2018), Lattice-Boltzmann method, 2D planar simulations
 - Xie et al. (2017), VOF method, drop impact in film of annular flow, 3D simulation
 - Gupta & Kumar (2020), deep liquid pool, interFoam, 3D simulation →




 M. Chai, K. Luo, C. Shao, S. Chen, J. Fan, DNS analysis of incipient drop impact dynamics using an accurate level set method, *Chin. J. Chem. Eng.* **25** (2017) 1-10
 C. Liu, M. Shen, J. Wu, Investigation of a single droplet impact onto a liquid film with given horizontal velocity, *Eur. J. Mech. - B/Fluids* **67** (2018) 269-279
 Z.H. Xie, G.F. Hewitt, D. Pavidis, P. Salinas, C.C. Pain, O.K. Matar, Numerical study of three-dimensional droplet impact on a flowing liquid film in annular two-phase flow, *Chem. Eng. Sci.* **166** (2017) 303-312
 G. Gupta, P. Kumar, Splashing dynamics of a drop impact onto a deep liquid pool with moving film interface, *Phys. Fluids* **32** (2020) 012102

Drop impact on film of immiscible liquid

Dyed water droplet impacting an oil film (exp.)

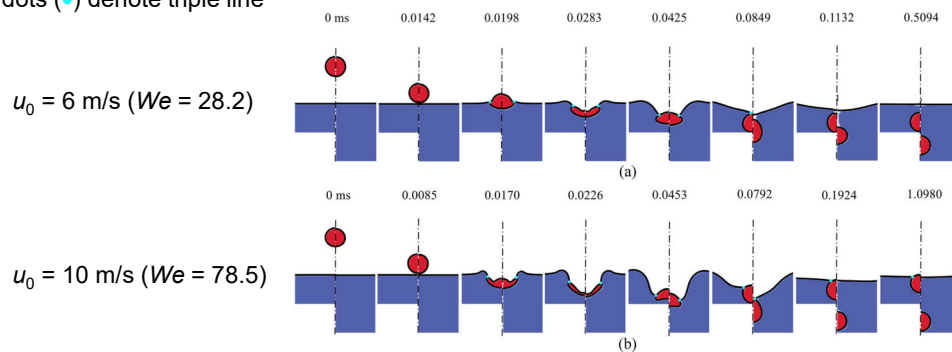


 S. Shaikh, G. Toyofuku, R. Hoang, J.O. Marston, Immiscible impact dynamics of droplets onto millimetric films, *Exp. Fluids* **59** (2017) 7

 H. Kittel, I. Roisman, C. Tropea, Splash of a drop impacting onto a solid substrate wetted by a thin film of another liquid, *Phys. Rev. Fluids* **3** (2018) 073601

Water droplet impact onto an oil layer (sim.)

- Three immiscible fluids (water, oil, air → three interfacial tensions and triple line of fluids)
- Extended *Gerris* code
 - Three-phase geometric VOF method (PLIC, two volume-fraction fields)
 - Axisymmetric simulations, $d_{\text{drop}} = 56.6 \mu\text{m}$, $\mu_{\text{drop}} / \mu_{\text{film}} = 4$, $h_{\text{film}} / d_{\text{drop}} = 1.5$ (left) and 3 (right)
 - Cyan dots (•) denote triple line



B. Wang, C. Wang, Y. Yu, X. Chen, Spreading and penetration of a micro-sized water droplet impacting onto oil layers, *Phys. Fluids* **32** (2020) 012003

Drop impact on film of miscible liquid

Drop impact on film of a miscible liquid

- Miscibility effects
 - “Interfacial tension” between miscible liquids which diminishes over time (Smith et al. 1981)
 - Contact angle changes in time (Chen et al. 2017) →
- Literature status
 - Only very few experimental studies (see below)
 - Drop-wall interaction of miscible liquids is not understood and a numerical method which can capture the above miscibility effects has not been developed so far

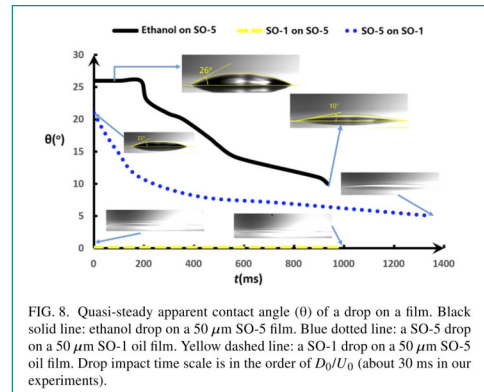


FIG. 8. Quasi-steady apparent contact angle (θ) of a drop on a film. Black solid line: ethanol drop on a $50\ \mu\text{m}$ SO-5 film. Blue dotted line: a SO-5 drop on a $50\ \mu\text{m}$ SO-1 oil film. Yellow dashed line: a SO-1 drop on a $50\ \mu\text{m}$ SO-5 oil film. Drop impact time scale is in the order of D_0/U_0 (about 30 ms in our experiments).

P. G. Smith, T.G.M. Vandeven, S.G. Mason, The transient interfacial tension between two miscible fluids, *J. Colloid Interf. Sci.* **80** (1981) 302-303
 N. Chen, H. Chen, A. Amirfazli, Drop impact onto a thin film: miscibility effect, *Phys. Fluids* **29** (2017) 092106
 N. E. Ersoy, M. Eslamian, Capillary surface wave formation and mixing of miscible liquids during droplet impact onto a liquid film, *Phys. Fluids* **31** (2019) 012107
 A. Geppert, A. Terzis, G. Lamanna, M. Marengo, B. Weigand, A benchmark study for the crown-type splashing dynamics of one- and two-component droplet wall-film interactions, *Exp. Fluids* **58** (2017) 172

Research topics in SFB-TRR/150

- “Turbulent, chemically reactive, multi-phase flows near walls” (Speaker A. Dreizler, TU Darmstadt)
- Interaction of fuel spray droplets impacting onto lubricating oil films on the cylinder walls results in splashing of mixed component droplets into the combustion chamber
 - Drop and wall consist of different but miscible liquids
- Injection of urea-water-solution (UWS) into the exhaust gas system of Diesel vehicles for selective catalytic reduction of NOx
 - Effect of UWS injection is influenced by UWS film existing on the wall
 - Drop and wall consist of solutions with different concentrations
- Project B08 (H. Marschall, M. Wörner)
 - “Numerical simulation of drop-wall interaction of miscible liquids”
 - Extensions of code *phaseFieldFoam*



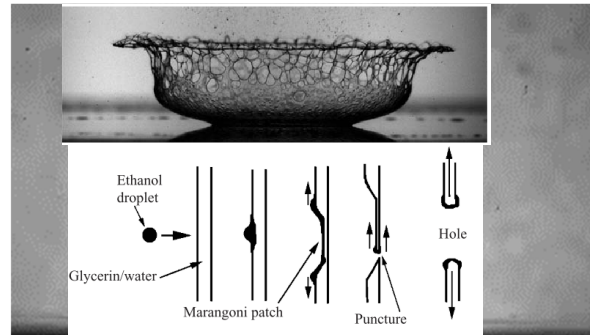
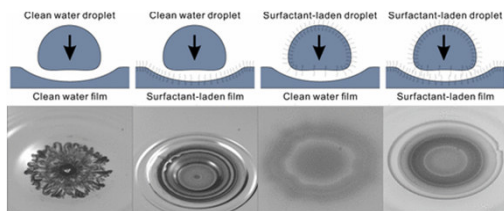
SFB/Transregio 150
Turbulente, chemisch reagierende
Mehrphasenströmungen in Wandnähe



Milad Bagheri

Surfactant-induced Marangoni effects (exp.)

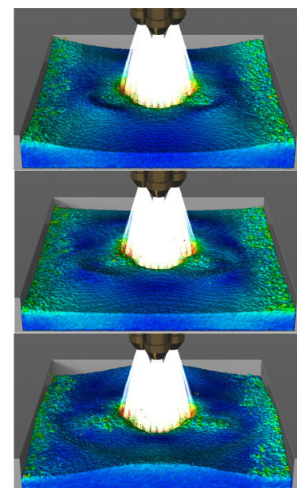
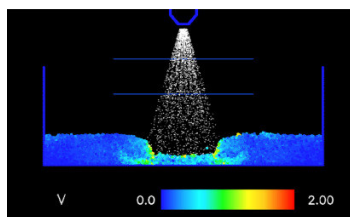
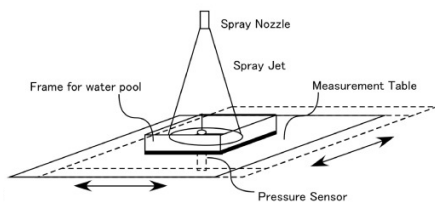
- Surfactants can significantly effect the impact process by changing the local surface tension giving rise of Marangoni stresses driving flow in the direction of higher surface tension
- Surfactants alter propagation of capillary waves, crown evolution and formation of secondary droplets (Che & Matar 2017)
- Crown breakup by Marangoni instability



Z. Che, O.K. Matar, Impact of Droplets on Liquid Films in the Presence of Surfactant, *Langmuir* **33** (2017) 12140-12148
 S.T. Thoroddsen, T.G. Etoh, K. Takehara, Crown breakup by Marangoni instability, *J. Fluid Mech.* **557** (2006) 63-72

Spray impingement into a liquid pool

- Coupled DEM-SPH simulation
 - The spray is represented by discrete particles which can collide with the wall, each other and also merge with liquid surfaces
 - The liquid pool dynamics are solved by SPH method
 - Coupling allows momentum transfer from the discrete spray into the pool liquid



P.W. Cleary, Y. Serizawa, A coupled discrete droplet and SPH model for predicting spray impingement onto surfaces and into fluid pools, *Appl. Math. Mod.* **69** (2019) 301-329

Conclusions



Achievements

- The level of details that can be captured nowadays by advanced numerical methods and computer codes is far beyond what one could imagine two decades ago
- Dynamic adaptive grid refinement is essential to bridge the gap of length scales
- Series of DNS simulations serve to gain fundamental understanding and develop regime maps

Limitations

- Many simulations consider idealized situations not encountered in practice, however, even for idealized situations modeling of details of impact dynamics is still challenging in 3D
- Results for splashing by crown formation depend on grid resolution and further numerical parameters → methods are not predictive yet
- Dynamic contact angle modelling and pinning due to topological or chemical heterogeneities of solid surface
- Influence of surfactants and miscibility

Acknowledgements



Development *phaseFieldFoam*

- *Xuan Cai*, Martin Wörner
- Holger Marschall (TU Darmstadt)
- *Andrea Schillaci*
- *Michael Holzinger* (TU Darmstadt)
- Nima Samkhaniani
- Abdolrahman Dadvand
- Milad Bagheri (SFB/TRR-150)

Code application

- Alexander Stroh (KIT, ISTM)
- *Verena Fink*
- *Ronan Bernard*
- *Farshid Jamshidi*
- *Arijit Majumdar*
- *Shuo Wang*
- *Yanchen Wu*

